ELSEVIER

Journal of Chromatography A, 924 (2001) 111–122

JOURNAL OF CHROMATOGRAPHY A

www.elsevier.com/locate/chroma

Experimental demonstration of the possibility to perform shear-driven chromatographic separations in micro-channels

Gert Desmet*, Nico Vervoort, David Clicq, Gino V. Baron

Vrije Universiteit Brussel, Department of Chemical Engineering, Pleinlaan 2, 1050 Brussels, Belgium

Abstract

The possibility to perform shear-driven chromatographic separations in micro-channels is demonstrated, using a novel laser-jet printed microfluidic channel system. The obtained theoretical plate numbers are in fair agreement with the theoretical calculations. Theoretical extrapolations of the separation speeds and detection limits which can be achieved when further miniaturizing the current system are presented as well.

Keywords: Shear-driven chromatography; Instrumentation; Dyes

1. Introduction

The past decade has witnessed a strong interest in the acceleration and miniaturisation of analytical separation processes [1–7]. In a theoretical performance study [8], we already pointed out the large gains in separation speed and separation resolution which can be obtained when switching from a pressure-driven to a shear-driven mode for the propulsion of the mobile phase flow in chromatographic systems. The technique, referred to as shear-driven chromatography (SDC), evades the pressure drop limitation of pressure-driven chromatographic systems and therefore enables the use of channels with a (kinetically advantageous) sub-μm thickness d, without any restriction on the applicable mobile phase velocity [9]. The increased separation speed then follows directly from the well-established fact [10] that, in any chromatographic system which is not pressure-drop limited and which hence allows one to establish a sufficiently large mobile phase velocity, the retention time t_R can be reduced according to $t_R \sim d^2$, where d is the characteristic radial diffusional distance and where it is assumed that the stationary phase thickness is scaled down in a linearly proportional way with d.

As shown in Fig. 1, the SDC principle is based on the use of channels which are divided into two, non-sealed and independently movable parts. By axially sliding the two parts relative to each other, and by relying on the viscous effect which exists in

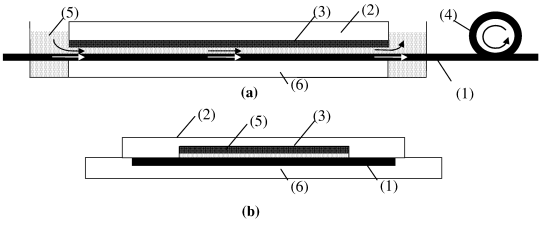

Fig. 1. Schematic layout of a basic shear-driven chromatographic system: longitudinal (a) and cross-sectional view (b). Description of the different parts: (1) moving wall element, (2) stationary wall element carrying the stationary phase layer (3), (4) motor, (5) mobile phase liquid, (6) glass support plate.

*Corresponding author. Tel.: +32-2-6293-251; fax: +32-2-6293-248.

E-mail address: gedesmet@vub.ac.be (G. Desmet).

0021-9673/01/$ – see front matter
PII: S0021-9673(01)00773-7

every liquid, the moving channel element drags the mobile phase liquid through the channel, thereby establishing a net liquid flow without the need for a pressure or voltage gradient, only using the shear-force field originating from the moving wall element. As can be learned from basic hydrodynamics, the established flow displays a substantially linear velocity profile (see Fig. 2 and Ref. [9]). Shear-driven flows hence differ slightly from the conventionally used pressure-driven flows, where a parabolic velocity gradient is established. Shear-driven flows obviously also differ from the electrically-driven flows for example encountered in open tubular capillary electrochromatography (CEC), where a perfectly flat velocity profile is established. However, when using channels or columns with a sufficiently small radial dimension, the peak broadening effect of the velocity gradient can be wiped out to a large extent by the molecular diffusion in the radial direction. It can furthermore be shown theoretically that the impact of the exact shape of the velocity profile on the peak broadening is only of secondary importance [8]. Accounting for the presence of the linear velocity gradient, the theoretical plate height expression for a shear-driven flow through an open tubular channel with a flat-rectangular cross-section can be shown to be given by [8]:

$$H = 2 \cdot \frac{D_m}{u} + \frac{2}{30} \cdot \frac{1 + 7k + 16k^2}{(1+k)^2} \cdot u \cdot \frac{d^2}{D_m} + \frac{2}{3} \cdot \frac{k}{(1+k)^2} \cdot u \cdot \frac{d_f^2}{D_s} \quad (1)$$

The absence of a pressure drop in SDC can be understood from the fact that in SDC the flow generating force is applied all along the column length [in fact similar to the generation of an electroosmotic flow (EOF)], whereas in a pressure-driven system the flow generating force is only applied on the (extremely small) column inlet surface, leaving the entire internal column wall surface to act as a flow resistance.

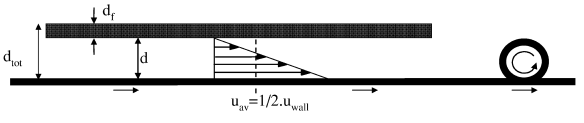

Fig. 2. Schematic representation of the flow profiles in a shear-driven flow.

With respect to CEC, the advantage of SDC resides in the fact that the fluid velocity does not depend upon a variable and sensitive parameter such as the magnitude of the zeta-potential at the channel wall surface, but is purely controlled by mechanical means. The established flow-rates are hence perfectly predictable and reproducible: it can be demonstrated, both theoretically [8] and experimentally [9], that the established fluid velocity in SDC always exactly equals one half of the imposed moving wall velocity, independently of the viscosity and the composition (pH, conductivity, etc.) of the liquid. The SDC concept hence offers a fundamental way to get round the fluid composition dependence of the migration times in CEC [11,12].

In a previous study [9], we have already demonstrated the possibility to generate high-speed low-dispersive flows through channels as thin as 100 nm and at velocities up to 2 cm/s (corresponding to a required inlet pressure of over 3000 bar in a pressure-driven system). The present paper reports on the realization of the first actual shear-driven chromatographic separations. To facilitate the detection, and in order to be able to perform the separations with commercially available reversed-phase high-performance liquid chromatography (RP-HPLC) beads, the relatively thick channels (8 to 20 μm) had to be used. To outline the potential of the SDC system, we also present a theoretical extrapolation of the separation speeds and detection limits which can be expected when reducing the channel thickness.

2. Experimental

2.1. Experimental set-up and flow channel manufacturing

A set-up similar to the set-up described in Ref. [9] was built. Although we already extensively demonstrated [9] the possibility to realize shear-driven flows in glass channels as thin as 100 nm and manufactured by means of reactive ion etching (RIE), all experiments in the present study were conducted in so-called laser-jet printed channels.

These channels were preferred over the more precisely machined RIE-etched glass channels, because of the low cost and the ease with which they can be produced, and because they allow the use of conventional microscope slides as the support for the stationary phase coating (see Fig. 3). This low-cost approach allowed us to explore different coating procedures in a relatively fast and cheap way. For the printing process a commercial laser-jet printer (Hewlett-Packard LaserJet 1100 with a HP-C4092A toner cartridge) was used to print two arrays of parallel toner particle lines over the entire length of a conventional transparency sheet (see Figs. 3 and 4). Closing the thus obtained half-open channels by putting a conventional microscope slide, carrying the stationary phase layer, on top of the printed toner lines, a ready-to-use and very cheap SDC channel system is obtained (Fig. 3b). The printed toner lines serve at the same time as side walls to delimit the lateral extent of the channel, and as spacers to maintain a given height difference between the bottom and the top wall. Putting the microscope slides traverse to the printed lines, the presently investigated channels had a length of 25.4 mm. A simplified top view of the set-up is given in Fig. 4.

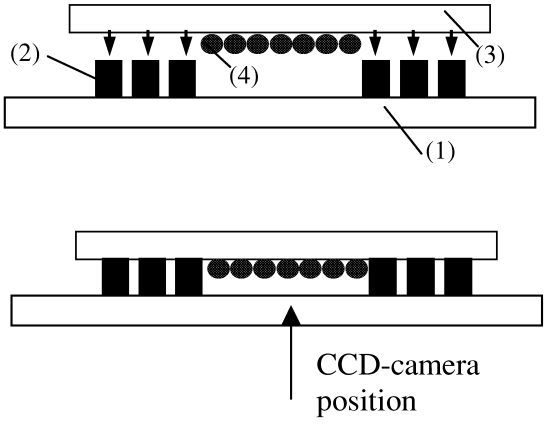

Fig. 3. Cross-sectional view (not to scale, see text) of a laser-jet printed shear-driven chromatography channel prior to assembly (a) and after assembly (b). The channel consists of a plastic sheet (1) coated with two parallel strips of carbon particles (2) and covered with a microscope slide (3) partially coated with a mono-layer strip of porous HPLC particles (4). During the operation, the plastic channel sheet moves in a direction perpendicular to the drawing (cf. Fig. 4). The printed side walls (2) of course move along with the plastic sheet (1).

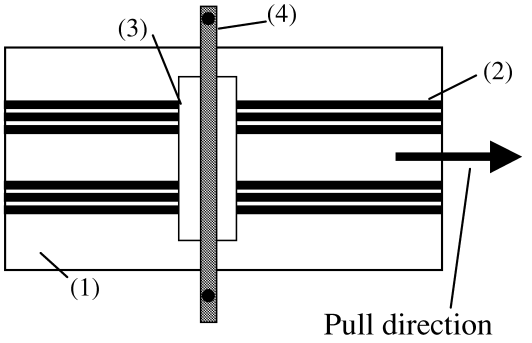

Fig. 4. Top view of a basic shear-driven chromatography system. During the operation, the plastic sheet (1) carrying the printed channel side walls (2) is pulled underneath the microscope slide (3) carrying the stationary phase layer. The microscope slide is held stationary with a fixation frame (4).

The stripe pattern design of the side walls was inspired by our concern to have a minimal contact area between the moving and the stationary channel parts, while still providing a sufficient support surface to avoid sagging of the microscope slide. The height of the printed channel side walls was measured with a Talystep apparatus (Rank Taylor Hobson, UK).

2.2. Coating of the microscope slides

As the main component of the stationary phase, we used commercial RP-HPLC beads (Superspher 100, RP-18-endcapped; Merck, Darmstadt, Germany) with a nominal mean diameter $d_p = 4$ μm. To immobilize the beads onto the microscope slides forming the upper wall of the channels, a polyacrylic polymer matrix was used. Prior to the application of the coating solution, the microscope slides where cleaned with an aqueous detergent solution and rinsed thoroughly with deionized water. Etching of the microscope slides for maximally freeing the silanol groups on the glass surface was done by treatment with 1 *M* KOH for 3 h and 0.03 *M* HCl for 1 h and rinsing the slides sufficiently with deionized water. Subsequently, the glass slides were surface treated by immersing them overnight in a 20% (v/v) solution of 3-(trimethoxysilyl)propyl methacrylate (Sigma–Aldrich, Belgium) in toluene. After this step, the slides were rinsed with toluene and acetone and dried with air. Then, 50 μl of a mixture

consisting of 25% (w/w) trimethylolpropane trimethacrylate (Sigma–Aldrich) and *x*% (w/w) of the RP-HPLC beads dissolved in a mixture of toluene–octane (80:20, v/v) was spotted on one of the surface treated microscope slides. During the experiments, *x* was varied between 0.5 and 25% (w/w). Prior to the application, the mixture was thoroughly sonicated during 5 min at 375 W and 20 kHz with a CV17 sonicator from Sonics & Materials (USA). The mixture also contained 1% (w/w of the monomer mass) benzoin methyl ether (Sigma–Aldrich), serving as the initiator for the photopolymerization reaction. The toluene–octane mixture acted as a porogen agent [13] to make the polymer matrix sufficiently porous, to enable a swift mass transfer of the sample species through the matrix. The ratio of toluene–octane (80:20) proved to yield the layers with the highest separation resolution. After spotting it, the droplet was smeared out over the entire microscope slide by putting a second, untreated microscope slide on top of it, and firmly pressing the two slides together. The untreated microscope slide was used to prevent diffusion of oxygen into the monomer mixture and to prevent evaporation of the solvent. Polymerization was achieved by irradiation of the slide sandwich system with UV light (365 nm) for 30 min. During the polymerization, a mass of about 500 g was applied on top of the slide sandwich. After 2 h, the two slides were separated with a razor blade, leaving the stationary phase only on the surface treated slide. After rinsing the stationary phase with toluene and methanol, the layer was dried with air and ready for use. As a final step, the coating was removed from the major part of the slide, again with a razor blade, leaving only a narrow lane of coating fitting into the space between the two printed side walls.

2.3. Flow generation, separation and detection

The generation of the mobile phase flow simply occurred by moving the plastic channel sheet underneath the microscope slide (cf. Fig. 4). The motion of the plastic channel sheet was effected either manually or motor-driven, and required only a negligible force (order 0.01 N). The investigated fluid velocities ranged between 0.1 mm/s and 2 cm/s.

For the separation experiments, a binary mixture of Rhodamin B and a food ink, PN Black 151 (CAS No. 2519-30-4; Sigma–Aldrich), was considered. When injected at a 10 m*M* concentration, the flow of the two dyes could be clearly monitored with a CCD camera (SONY DXC-950P) equipped with a zoom lens and positioned underneath the transparent channel bottom wall (see Fig. 3a). The images were captured with a DC10 video capture card (Pinnacle Systems, Germany). At regular intervals, still images were taken and colour intensity plots were made with a commercial photo-editing package (MS Photo Editor), using a self-written Mathlab-routine to automate the process. The rather unusual detection method (charge coupled device (CCD) camera) was preferred during the present initial experimental phase, because it offers a visual control over the ongoing separation, providing for example information on disturbances of the flow due to occasional protuberances from the coated layers. Current work is underway to couple the SDC channels to a laser induced fluorescence (LIF) detection system. The procedure for the injection of the sample mixtures is represented in Fig. 5. Using the still-images, the retention factor k of the two dyes could be derived from the difference between the position L_0 of a virtual line representing the velocity of the non-retained mobile phase liquid (moving with exactly one half of the moving wall velocity), and the actual position L_{eff} of the moving dye peak, using:

$$k = \frac{L_0 - L_{\text{eff}}}{L_{\text{eff}}} \tag{2}$$

The elaboration of the method for the determination of k is represented in Fig. 7. From the peaks in the color intensity plots, estimates of the theoretical plate height could be made, using the difference between the variance $\sigma^2_{x,\text{inj}}$ of the injected peak and the variance σ^2_x of the peak after having elapsed a given distance L_{eff}, using [14]:

$$H = \frac{\sigma^2_x - \sigma^2_{x,\text{inj}}}{L_{\text{eff}}} \tag{3}$$

As the mobile phase liquid, a wide range of water–methanol was considered. All the experiments were performed at ambient temperature ($T \cong 20^\circ\text{C}$).

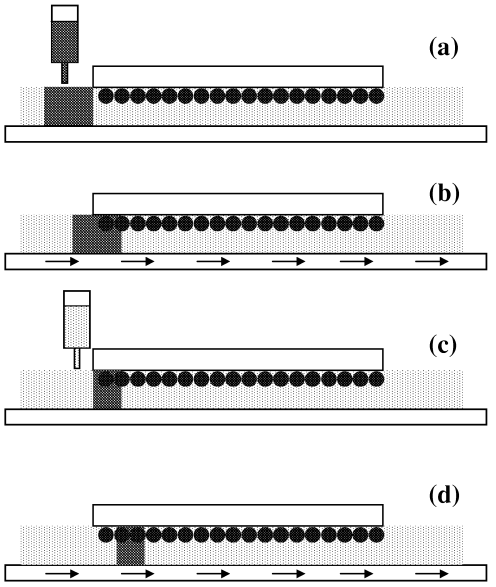

Fig. 5. Schematic representation (longitudinal view – not to scale) of the injection procedure. First, a small amount of the sample liquid is put in front of the channel inlet with a conventional liquid syringe (a). Then, the channel sheet is slightly displaced in order to fill approximately the first 300 to 500 μm of the channel with the sample (b). Subsequently, the non-entered sample is flushed away (c), and the motion of the channel sheet is resumed (d).

3. Results

The Talystep measurements of the nominal height of the printed toner particle lines yielded a value of about 8 μm (±0.2 μm), very consistently along the entire length of the channel. This height measurement was confirmed with a scanning electron miscroscopy (SEM) picture study, revealing that the printing lines consist of a dense monolayer of relatively uniform sphere-like carbon particles, with a maximal diameter of the order of 8 μm.

Using the capillary force effect, the laser-jet printed SDC channels filled up automatically, simply by putting a drop of the mobile phase liquid near one end of an empty channel. This self-filling action typically only took about 5 (thinnest channels) to 10 s (thickest channel), and could furthermore easily be accelerated by axially displacing the movable wall plate during the filling process. The printed channels could typically be used for about 20 consecutive runs, at least when aqueous liquids were used: when highly hydrophobic liquids such as 1-octanol were used, an excessive wear of the side walls was observed, because the printer toner particles dissolved easily in the octanol.

An SEM picture of one of the stationary phase layers obtained by the polyacrylic coating technique is shown in Fig. 6. The picture is taken at a position where the layer was accidentally cracked, providing a good view of how the RP-HPLC beads are contained within the polyacrylic matrix. As we always applied the same mass during the photopolymerization process, the thickness of the layer was found to be especially a function of the mass fraction of the RP-HPLC beads in the coating mixture. Above 5% (w/w), the beads heaped up in layers exceeding the monolayer thickness, below 5% (w/w), the layer thickness was of the same order as the monolayer thickness (approximately 4.5 μm), but the surface coverage of course decreased with decreasing mass fraction. Most of the layers we produced were similar to the one shown in Fig. 6, i.e., the particles were fully contained within the polymer matrix.

Fig. 7 presents two still-images of a CCD-video recording of a typical separation experiment, showing that the two dyes are separated within 17 s and after having elapsed a distance of less than 5 mm. For a clear understanding of the photographs, it should be noted that the images are taken through the transparent bottom channel wall, and that the

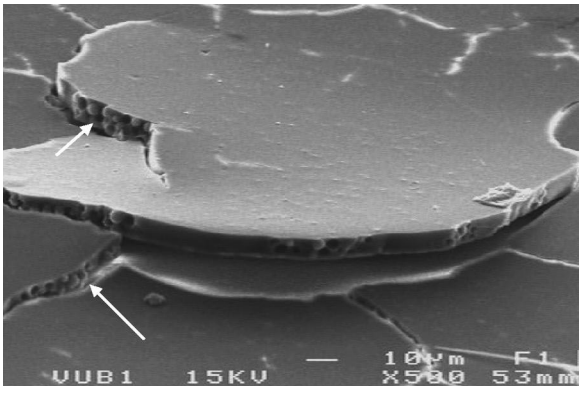

Fig. 6. SEM picture of one of the prepared stationary phase coatings (used in the separation presented in Fig. 10), offering a view on the internal structure of the polymer matrix surrounding the RP-HPLC beads. The white arrows indicate a position where the RP-HPLC beads are clearly visible.

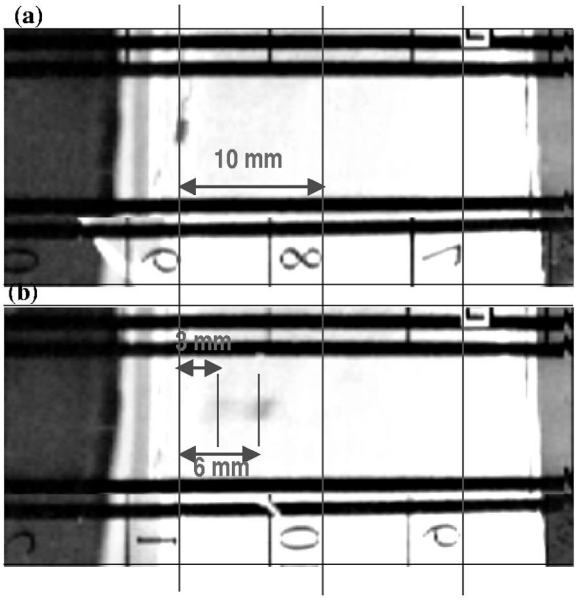

Fig. 7. Photographic images, respectively, taken at $t=0.0$ s (a) and $t=17$ s (b), of a chromatographic separation of a Rhodamin B/PN Black 151 mixture. Coating prepared with a 5% (w/w) fraction of the RP-HPLC beads. Side wall height $=d_{tot}=8$ μm. Mobile phase liquid thickness: $d=4$ μm. Stationary phase thickness: $\delta=4$ μm. Mean fluid velocity $=0.2$ mm/s. Mobile phase: methanol–water (30:70, v/v).

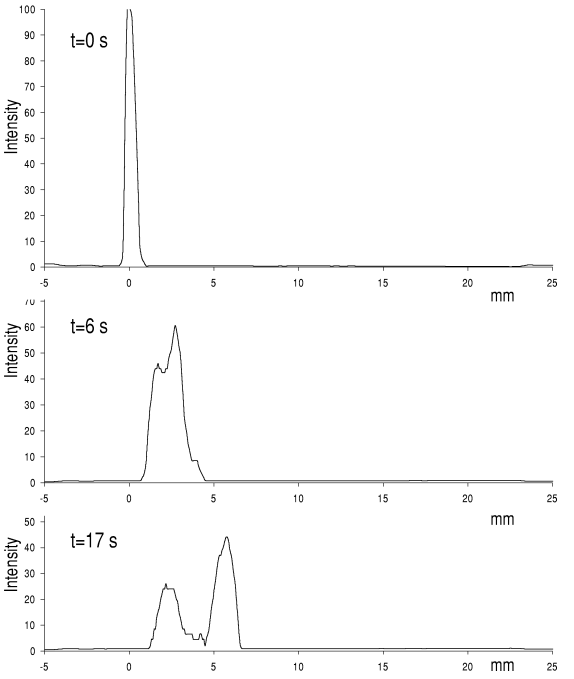

Fig. 8. Sequence of colour intensity plots describing the course of the separation presented in Fig. 7.

numbered transversal black reference lines are spaced by exactly 10 mm, and are used to visualize the movement of the moving wall. From the sequence of photographs, it can clearly be seen that the dye plugs move through the channel in a purely uni-directional manner, without the occurrence of flow disturbances. This was the case in most of our experiments. Occasional deviations could always be explained from defects in the stationary phase layer.

Making a color intensity plot along a given pixel line of a number of still images taken during the separation shown in Fig. 7, the evolution of the separation can be clearly followed (Fig. 8). Fig. 9 shows the evolution of a separation performed in a channel using a stationary phase prepared without prior sonication of the coating slurry. The peak broadening obviously is much larger than in the case presented in Fig. 8, and the peaks only become separated near the end of the channel. Although the solid mass fraction in the coating mixture was similar to the one used for the layer used in the experiment presented in Fig. 8, SEM pictures of the layer showed that he thickness of the layer was much larger, very irregular, with peaks as high as 16 μm, and with a mean thickness of the order of 12 μm. Given the thickness of the layer, we were forced to use the layer in combination with a triple printed channel sheet. Given that the total thickness in a triple printed channel is about $d_{tot}=20$ μm, the use of a layer with mean thickness $d_f=12$ μm implies that the mobile phase fluid layer was about 8 μm thick

In Fig. 10, a separation with the layer shown in Fig. 6 is presented. With a stationary phase thickness estimated to be about 6 to 7 μm, implying that the mobile phase fluid layer is about 1 to 2 μm thick when used in a channel with a side wall height of $d_{tot}=8$ μm, the represented case corresponds to a separation with an unusually large phase ratio. As can be denoted, the separation occurs within a few mm.

A summary of the experimental data is presented in Table 1. The retention values were estimated in a manner similar to Fig. 6, and the theoretical plate

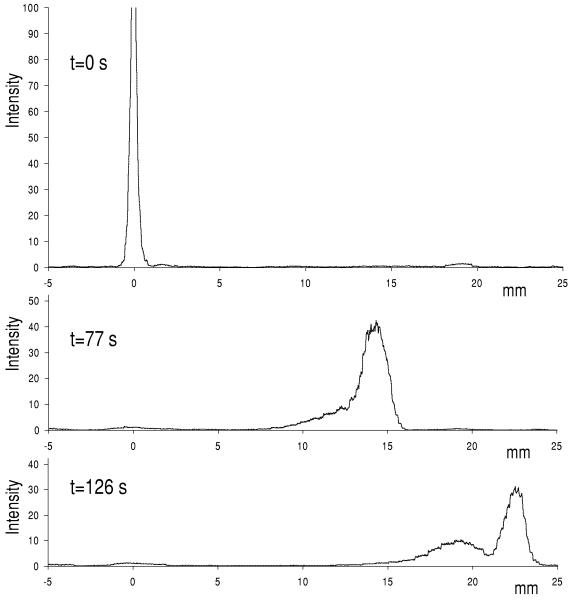

Fig. 9. Sequence of colour intensity plots describing the course of a shear-driven chromatographic separation of a Rhodamin B/PN Black 151 mixture. Coating prepared with a 5% (w/w) fraction of the RP-HPLC beads (coating applied without preceding sonication). Side wall height = d_{tot} = 20 μm. Mobile phase liquid thickness: d = 8 μm. Stationary phase thickness: δ = 12 μm. Mean fluid velocity = 0.1 mm/s. Mobile phase: methanol–water (30:70, v/v).

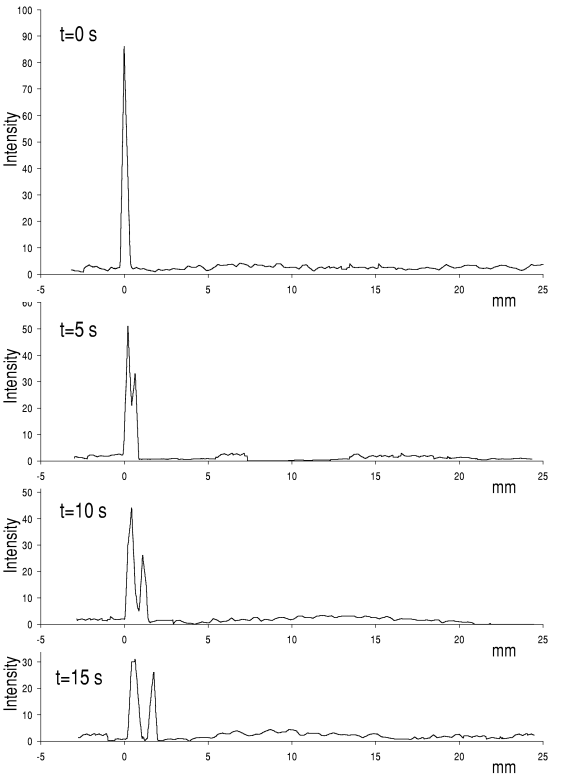

Fig. 10. Sequence of colour intensity plots describing the course of a shear-driven chromatographic separation of a Rhodamin B/PN Black 151 mixture. Coating prepared with a 15% (w/w) fraction of the RP-HPLC beads. Side wall height = d_{tot} = 8 μm. Mobile phase liquid thickness: d = 1.5 μm. Stationary phase thickness: δ = 6.5 μm. Mean fluid velocity = 0.1 mm/s. Mobile phase: methanol–water (90:10, v/v).

height values were obtained by applying Eq. (3) to the first eluting peak of the mixture. The theoretical plate heights were calculated using Eq. (1), with the parameter values as specified in the table. The liquid phase molecular diffusion coefficient of the Rhodamin B and PN Black dyes has been determined from independent experiments [15], and could be estimated to be of the order of $5 \cdot 10^{-10}$ m^2/s. As we had no independent measurements of the stationary phase diffusion coefficients, a rough estimate of $D_s = 5 \cdot 10^{-11}$ m^2/s was considered. Peak width data for component 2 are not given because the peaks are clearly not Gaussian, except perhaps in Fig. 10. At present, this can only be attributed to a secondary interaction between the Rhodamin and the polymer matrix used to immobilize the HPLC beads.

4. Discussion

The fact that the sample dye plugs move through the channel in a purely uni-directional manner, without the occurrence of sideways leakage flows, clearly shows that the open-architecture of the channels poses no specific problems. As already argued in Ref. [9], this is in agreement with the fact that, as the shear-driven flow generates no pressure drop or pressure build-up, convective leaks through the non-sealed channel side walls simply cannot occur.

The printing technique proves to be very flexible: the width of the channels could be freely chosen and was varied between 0.1 and 10 mm, and by repeating the printing process two or more times on the same sheet, the height of the side walls could be increased from about 8 μm (single printed channel), to about 14 μm (double printed channel) and 20 μm (triple

Table 1
Summary of experimental results

Experiment no.	Mobile phase composition methanol–water (%, v/v)	Beads in monomer mixture (%, w/w)	d_{tot} (μm)	d (μm)	d_f (μm)	V_s/V_m	k_1	k_2	u (mm/s)	H_{exp} (μm)	H_{theo} (μm)
(1) Fig. 7/8	30:70	5	8	4	4	1	0.7	2.3	0.2	55	14
(2) Fig. 9	30:70	5	20	12	8	1.5	1.0	3.0	0.1	105	46
(3) Fig. 10	90:10	15	8	6.5	1.5	4.3	0.2	2.1	0.1	18	13

Note: the H values correspond to the first eluting peak.

printed channel). The resulting column format, i.e., a channel with a flat rectangular cross-section (a few μm high and a few mm wide), allows to combine the fast separation kinetics offered by the relatively small radial diffusion distances with the large mass loadability offered by the large channel width. Another advantage is the open-architecture of the system, which, in combination with the cost-effectiveness of the stationary phase system, allows to use the stationary phases on a disposable basis. By printing the parallel lines over the entire length of an A4 sheet, a translation path length of about 30 cm is obtained. This means that, since the fluid is flowing at 1/2 of the moving wall velocity, the fluid volume present in a 2.5 cm long channel can be eluted approximately six times with a single passage of the A4 sheet. Modification of the technique to yield longer movable wall sheets is straightforward. Considering the rapid wear of the printed carbon particle lines when hydrophobic mobile phase liquids are used, a modification of the printing technique will also be necessary in order to enable normal-phase separations. This can however easily be achieved by replacing the carbon particles of the toner by particles of another material (e.g., non-porous silica or metallic beads). Another straightforward modification of the current technique is to switch to a different particle size. With only minor modifications it should also be possible to switch to toner particles for example of the order of 2 μ. Using such particles to form the channel side walls, and modifying the coating technique by switching for example to spherical HPLC particles of the order of 1 μm, it should hence be possible to down-scale the current system towards the 1 μm level in a relatively straightforward manner.

With the injection procedure depicted in Fig. 5, sharply delimited rectangular injection plugs with a width varying between 200 and 500 μm were obtained. Currently our set-up is being modified to control the displacement of the channel sheet with an automated displacement system (M-TS100 DC.5, Newport, The Netherlands). This will allow to control the axial width of the tracer plug with an accuracy of 0.5 μm. The fact that the flushing action for the removal of the non-entered sample does not disturb the entered sample plug, is simply due to the large pressure drop inside the thin SDC channels. In general, it can be said that the fact that the injections do not have to be applied against a pressure or a voltage gradient considerably facilitates the injection problem, and allows the use of relatively simple injection systems.

Comparing Figs. 8 and 9, it is obvious that sonication of the coating mixture was very critical in the present case. RP-HPLC apparently had a strong tendency to form agglomerates when dissolved in the monomer mixture. The current coating procedure, involving a lot of manual steps, is not very reproducible as yet. Differences in coating thickness and internal structure could clearly be observed from the SEM pictures. The coating to coating reproducibility of the separations was hence rather poor.

Currently, our coatings typically remain intact during 5 to 10 runs. Deterioration of the layers typically starts with the layer peeling off at one or more very localized positions. The debris is then carried along by the moving wall and scratches away larger portions of the coating. However, at least during the first five runs performed with each coating, the run to run reproducibility of the retention factors and the plate heights was always within the experimental error of a few %, as can be expected for a true LC system. The limited number

of experiments per coating however troubles a thorough statistical analysis.

The experimental retention factors in Table 1 are, within the experimental error, in agreement with the measured phase ratios (cf. entries in lines 1 and 2). For the experiment presented in Fig. 10 (experiment 3), the phase ratio was so large ($m \cong 4$) that we had to increase the strength of the mobile phase in order to have the Rhodamin B peak moving through the channel. The experimental theoretical plate heights presented in Table 1 are about 3- to 1.5-times larger than predicted by theory. This deviation can presumably be explained from the presence of the polymeric matrix, and/or from the occurrence of irregularities in the layer thickness. The fact that the particles are fully contained within the polymer matrix is of course undesirable from a chromatographic point of view, as is for example illustrated by the severe tailing of the peaks for component 2. The current coating method will hence obviously not be the method of choice for the future. Current work is undertaken to further reduce the channel thickness (including switching to the use of sub-μm porous beads), and to switch to other bonding methods. Two of these methods are: thermal bonding, and immobilization of the RP beads with a thin layer of polyethoxysilane (PES) which can be converted to silica upon reaction with an ammonia solution. This would allow to omit the polymer matrix surrounding the HPLC beads.

4.1. Theoretical detection and separation time limits of the SDC system

The present section is devoted to the calculation of the ultimate separation speeds and detection limits which can be achieved with the SDC concept. To put the calculated results in perspective, a comparison with HPLC is made. For the SDC system, the calculations are based on the theoretical plate height expression given in Eq. (1). For HPLC, the H values were calculated from [16]:

$$\mathrm{H} = \mathrm{A}d_\mathrm{p} + B \cdot \frac{D_\mathrm{m}}{u} + \frac{0.37 + 4.69k + 4.04k^2}{(1+k)^2} \cdot u \cdot \frac{d_\mathrm{p}^2}{D_\mathrm{m}} \tag{4}$$

using $A = 1$ and $B = 1.6$ as typical values. Following a procedure already outlined in [8], Eqs. (1) and (4) can be used together with Eqs. (5) and (6) to calculate the minimal analysis time required to perform a given separation in an SDC and in an HPLC mode:

$$t_\mathrm{R} = \frac{NH}{u} \cdot (1+k) \tag{5}$$

$$N = \frac{16R_s^2}{(1-\alpha)^2} \cdot \frac{(1+k)^2}{k^2} \tag{6}$$

For the SDC case, the mobile phase velocity u can be selected freely, and was consistently taken to be equal to 10 times the optimal mobile phase velocity, i.e., the velocity yielding the minimum H value in the Van Deemter plot corresponding to Eq. (1). For the HPLC case, the mobile phase velocity u was calculated such that it satisfies Poiseuille's law:

$$u = \frac{pd_\mathrm{p}^2}{\varphi \eta NH} \tag{7}$$

assuming an inlet pressure value of $p = 200$ bar and assuming a flow resistance factor of $\varphi = 750$. Taking typical values of $k = 3$ and $R_s = 1.25$, and varying α such that a whole range of N values is covered, Eqs. (4)–(6) have been used to numerically calculate the times t_R needed to perform a separation with given required N in a pressure-driven and a shear-driven mode (Fig. 11). For each N value, the mobile phase velocity u was calculated as explained above. Fig. 11 clearly illustrates the advantage of a shear-driven operation: the steep increase of the HPLC curves for large N is a direct consequence of the pressure-drop limitation, an observation which is in agreement with the considerations in [17]. The SDC curves do not display this steep increase and vary according to $t_\mathrm{R} \sim Nd^2$ over the entire range of N. Fig. 11 also clearly shows that, whereas in a pressure-driven system such as HPLC, a reduction of the characteristic diffusional distance from $d_\mathrm{p} = 3$ μm to $d_\mathrm{p} = 1$ μm is counter-productive and leads to an increase of the analysis time for all separations with $N > 5000$, the effect of a similar miniaturisation of the SDC system is purely positive and leads to a monotonic decrease of the required analysis time. As can be denoted, the SDC system allows for an even further increase of the analysis speed, i.e., by further decreasing the channel thickness towards the $d = 0.1$-μm range.

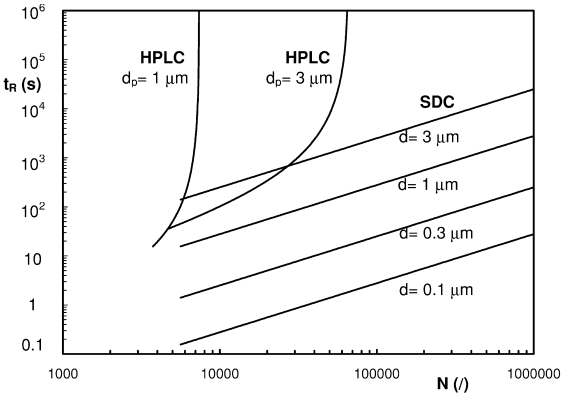

Fig. 11. Comparison of the required analysis time in HPLC and SDC as a function of the required theoretical plate number. All points along the presented curves correspond to a critical pair separation with $k=3$. The molecular diffusivity in the mobile phase was taken to be $D_m=1\cdot10^{-9}$ m^2/s. The HPLC data were obtained by calculating u from Eq. (7) with $p=200$ bar, $\varphi=750$, $\eta=1\cdot10^{-3}$ kg/m s and by putting $A=1$, $B=1.6$ in Eq. (4). For the SDC case, it was assumed that $D_s=5\cdot10^{-10}$ m^2/s, $\delta=d/10$ and $u=10\cdot u_{opt}$.

As the major bottleneck of so-called rapid chromatographic systems [e.g., open tubular (OT) LC or OT-CEC] is usually found in their lack of mass loadability (and the correspondingly poor concentration sensitivity), we have also calculated the maximum detectability of the SDC system and compared it to that of HPLC, which is generally considered to be the chromatographic system yielding the lowest detection limits. For this comparison, the maximal peak concentration of the eluting components was calculated using an expression taken from Tock et al. [18]:

$$C_{max}=\frac{m_{30}\rho_{sf}}{M_r}\cdot\frac{1}{\sqrt{2\pi N}}\cdot\frac{1+k}{k^2}\cdot\frac{V_s}{V_m} \quad (8)$$

For the SDC system, the volumetric phase ratio $m=V_s/V_m$ is given by $m=V_s/V_m=d_f/d$, and can hence be freely selected, whereas in the packed columns used in HPLC and in CEC, the volumetric phase ratio m is a non-freely selectable variable $[m=V_s/V_m=(1-\epsilon)/\epsilon]$ and is approximately equal to $m=V_s/V_m\cong1.5$ (assuming that $\epsilon=0.4$). Considering now Fig. 12, where the analysis times of HPLC and SDC are compared as a function of d ($=d_p$ for the HPLC case) for a separation with a given required N, it can clearly be denoted that, when for example considering an SDC system with $d=0.2$ μm, the thickness of the stationary phase layer can be increased up to a value of $m=d_f/d=20$, while still requiring only an analysis time which is about two times shorter than in the best possible HPLC system. Considering that $C_{max}\div V_s/V_m$ (Eq. (8)), this observation implies that in an SDC system with an optimally designed phase volume ratio, the peaks can elute from the column at a concentration which is roughly 10 times larger than in the best possible HPLC system ($V_s/V_m=20$ for SDC against $V_s/V_m=1.5$ for HPLC), while still retaining some of the increased separation speed of SDC.

Considering now a UV absorption detection scheme with a laser beam guided through the side walls of the SDC channel, the optical path length in the SDC system is dictated by the lateral width of the channel, allowing to maximally benefit from the increased elution concentrations. It should be noted here that the laser beam detection in the SDC channels should of course preferentially occur at a position where the stationary phase is locally re-

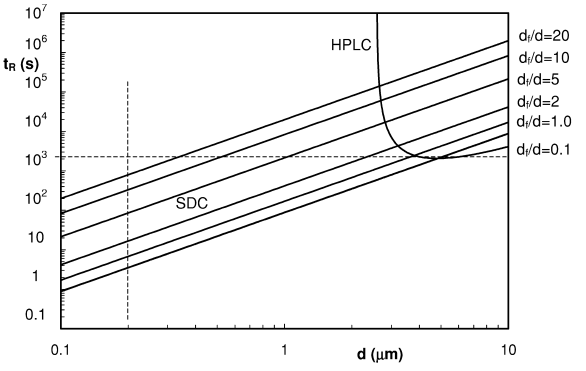

Fig. 12. Comparison of the required minimal analysis time in HPLC and SDC as a function of the characteristic diffusional distance (d_p for HPLC, and channel diameter d for SDC), and for different values of the phase volume ratio β. All points along the presented curves correspond to a critical pair separation with $k=3$, $R_s=1.25$ and $\alpha=1.03$, or, equivalently, $N\cong49\,400$. The other parameters were similar to those in Fig. 11.

moved, such that a gap of few μm in diameter is available for the passage of the laser beam. Considering the factor 10 in concentration gain, and considering that a lateral channel width (and a corresponding optical path length λ) of a few mm is perfectly feasible with the SDC system (cf. the presently used channel layout), and comparing this to a typical optical path length of $\lambda = 5$ mm for the HPLC system, it is obvious that the factor 10 in concentration gain of the SDC system is more than sufficient to lead to $C_{max}\lambda$ values surpassing those of HPLC. According to Beer–Lambert's law (detectability $\div C_{max}\lambda$), this implies that the SDC system has the potential to offer lower detection limits than HPLC.

5. Conclusions

With a relatively rudimentary, self-developed coating procedure, a functioning shear-driven chromatographic separation apparatus has been built and a series of chromatographic separations could be effected, without the assistance of a pressure- or voltage-gradient, using the shear-force field originating from a moving column part as the single source of momentum for the propulsion of the mobile phase liquid. The deviations between the measured theoretical plate heights and the theoretically expected values is reasonable and is most probably due to the poor quality of the prepared stationary phase layers. The coatings also have a limited life time, which currently troubles a statistically sound method validation.

The presently investigated system obviously still has a large margin for improvement, both by enhancing the quality of the layers and by a further reduction of the channel thickness. The laser-jet channel printing technique provides an extremely cost-effective approach for the production of SDC channels, offering a large degree of freedom for the selection of the stationary to mobile phase volume ratio and, due to its cost-effectiveness, opening the road towards the use of stationary phases on a disposable basis. The performed theoretical analysis showed that the SDC technique not only finds a potential application in the performance of ultra-rapid separations, but that it also provides the opportunity (by applying the technique in sub-μm channels with phase ratios $>>1$) to yield detection limits which are comparable or even lower than those of HPLC.

6. Nomenclature

A,B	Constants in Van Deemter's equation, see Eq. (4), (mol/m^3)
d	Thickness mobile phase layer, see Fig. 2 (m)
d_f	Thickness mobile phase layer, see Fig. 2 (m)
d_p	Particle diameter (m)
d_{tot}	Total thickness of mobile + stationary phase layer, see Fig. 2 (m)
D	Molecular diffusion coefficient (m^2/s)
H	Height of equivalent theoretical plate (m)
k	Retention factor (–)
L_0	Migration distance of a non-retained component (m)
L_{eff}	Migration distance of a retained component (m)
m	Phase volume ratio, $m = V_s/V_m$ (–)
m_{30}	Reduced load, $m_{30} = 2$ [18]
M_r	Molecular mass of sample component, $M_r = 200$ g/mol [18]
N	Theoretical plate number (–)
p	Inlet pressure (bar)
R_s	Resolution factor (–)
t_R	Analysis or retention time (s)
u	Mean mobile phase velocity (m/s)
V	Phase volume (m^3)
x	Weight fraction of RP-HPLC beads in coating mixture (–)

Greek symbols

α	Separation factor (–)
δ	Stationary film thickness (m)
λ	Optical path length
η	Dynamic viscosity (kg/m s)
ρ_{sf}	Stationary phase density, $\rho_{sf} = 10^3$ kg/m^3 [18]
σ_x^2	Peak variance in the space domain (m^2)

Subscripts

m	Mobile phase
opt	Optimum
s	Stationary phase

Acknowledgements

We kindly acknowledge Professor Knut Irgum for his assistance with the development of the polyacrylic coating procedure. Part of this work has been supported by the IUAP 4-11 of the Belgian Federal Government.

References

[1] D.J. Harrison, K. Fluri, K. Seiler, Z. Fan, C.S. Effenhauser, A. Manz, Science 261 (1993) 895.
[2] B. He, N. Tait, F. Regnier, Anal. Chem. 70 (1998) 3790.
[3] M.M. McEnery, J.D. Glennon, J. Alderman, S.C. O'Mathuna, Biomed. Chromatogr. 14 (2000) 44.
[4] C. Ericson, J. Holm, T. Ericson, S. Hjertén, Anal. Chem. 72 (2000) 81.
[5] S. Matsui, Proc. IEEE 85 (1997) 629.
[6] H. Poppe, Analusis 22 (1994) 22.
[7] D. Figeys, Anal. Chem. 72 (2000) 330A.
[8] G. Desmet, G.V. Baron, J. Chromatogr. A 855 (1999) 57.
[9] G. Desmet, G.V. Baron, Anal. Chem. 72 (2000) 2160.
[10] G. Guiochon, Anal. Chem. 53 (1981) 1318.
[11] M.M. Dittmann, K. Wienand, F. Bek, G.P. Rozing, LC–GC Mag. 13 (1995) 800.
[12] W. Kok, in: Capillary Electrophoresis: Instrumentation and Operation, Chromatographia Suppl., Vol. 51, 2000, p. S-28.
[13] C. Viklund, E. Ponten, K. Irgum, Chem. Mater. 9 (1997) 463.
[14] K. Robards, P.R. Haddad, P.E. Jackson, Principles and Practice of Modern Chromatographic Methods, Academic Press, New York, 1994.
[15] S. Boogaerts, Masters Thesis, Vrije Universiteit Brussels, 2000.
[16] E.D. Katz, K. Ogan, R.P.W. Scott, in: F. Bruner (Ed.), The Science of Chromatography, Journal of Chromatography Library, Vol. 32, Elsevier, Amsterdam, 1985, p. 403.
[17] H. Poppe, J. Chromatogr. A 778 (1997) 3.
[18] P.P.H. Tock, C. Boshoven, H. Poppe, J.C. Kraak, J. Chromatogr. 477 (1989) 95.